

## Actuation of a suspended nano-graphene sheet by impact with an argon cluster

This article has been downloaded from IOPscience. Please scroll down to see the full text article.

2008 Nanotechnology 19 505501

(<http://iopscience.iop.org/0957-4484/19/50/505501>)

View [the table of contents for this issue](#), or go to the [journal homepage](#) for more

Download details:

IP Address: 128.143.22.132

The article was downloaded on 31/10/2011 at 14:01

Please note that [terms and conditions apply](#).

# Actuation of a suspended nano-graphene sheet by impact with an argon cluster

Norio Inui, Koza Mochiji and Kousuke Moritani

Graduate School of Engineering, University of Hyogo, 2167, Shosha, Himeji, Hyogo 671-2280, Japan

E-mail: [inui@eng.u-hyogo.ac.jp](mailto:inui@eng.u-hyogo.ac.jp)

Received 29 August 2008, in final form 14 October 2008

Published 24 November 2008

Online at [stacks.iop.org/Nano/19/505501](http://stacks.iop.org/Nano/19/505501)

## Abstract

Using a molecular dynamics simulation, we examine the actuation of nanodrums consisting of a single graphene sheet. The membrane of the nanodrum, which contains 190 carbon atoms, is bent by collision with a cluster consisting of 10 argon atoms. The choice of an appropriate cluster velocity enables nanometre deformation of the membrane in sub-picosecond time without rupturing the graphene sheet. Theoretical results predict that, if an adsorbed molecule exists on the graphene sheet, the quick deformation due to the impact with the cluster can break the weak bonding between the adsorbed molecule and the graphene sheet and release the molecule from the surface; this suggests that this system has attractive potential applications for purposes of molecular ejection.

(Some figures in this article are in colour only in the electronic version)

## 1. Introduction

Graphene, a single layer of graphite, has recently attracted attention not only for its unique electrical properties [1, 2] but also for its novel mechanical properties. A suspended graphene sheet, for example, is a promising candidate for membranes of nanodrums, which may be used in mechanical resonators designed for mass detection [3].

The actuation of the suspended graphene sheet [4] is a new technical subject. Bunch *et al* actuated a suspended graphene sheet by applying a time-varying radio-frequency to it [5]. We propose another method using a gas cluster ion beam, wherein the graphene sheet is actuated by collision with an argon cluster. The advantage of this method is that high pressure is generated locally in a very short time without the use of electrical circuits, although temporal control of the displacement is difficult. By using a cluster instead of a monomer as the source of kinetic energy, the kinetic energy per atom is decreased, and therefore the damage to the graphene sheet can be decreased.

The main purpose of this paper is to investigate the time evolution of the displacement of a graphene sheet after collision with an argon cluster. In particular, we consider the relation between the maximum displacement and several important parameters: the velocity of the cluster, the size of the cluster and the size of the graphene sheet. As an

application of the actuation of the graphene sheet, we examine the ejection of an adsorbed molecule from the graphene sheet. If the graphene is forced to move rapidly, the interaction between the adsorbed molecule and the graphene is broken, and the adsorbed molecule is released from the surface of the graphene. Thus, this technique allows the realization of a molecular injector, which may be used for manipulation in a nanochemical reactor or a mass spectrometer.

This paper is organized as follows. In section 2, we explain the method of the molecular dynamics simulation used to simulate the collision of the argon cluster with the graphene sheet. In section 3, we estimate the bending rigidity from the fundamental frequency of the graphene sheet using continuum mechanics. In section 4, we show the time dependence of the displacement of the suspended graphene after impact with argon for different impact speeds. We also consider the dependence of the deformation of the graphene sheet on the argon cluster size. In section 5, we show an application of our sheet method to molecular ejection. In section 6, we summarize the obtained results and discuss some of the problems encountered in the molecular dynamics simulation.

## 2. Simulation method

The collision of an argon cluster with a graphene sheet is simulated using a molecular dynamics (MD) method [6]. We

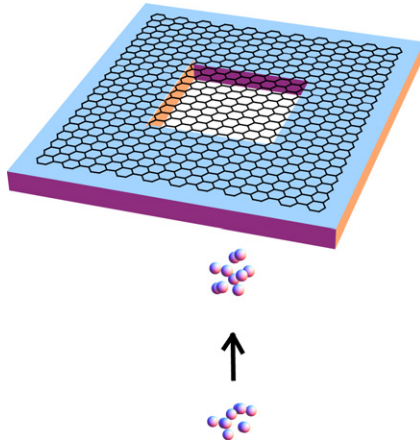


**Figure 1.** Schematic of actuation of the graphene sheet by collision with an argon atom. The graphene sheet is placed on a substrate having a square hole. The cluster collides with the graphene sheet vertically.

assume that a single layer of graphene is placed on a substrate with a square hole at the centre, as shown in figure 1. The argon cluster collides perpendicularly with the graphene sheet through the hole. To design this set-up, we referred to the recent experiment carried out by Poot and Zant [7]. They used a silicon wafer as the substrate, on which circular holes were etched with buffered hydrofluoric acid using resist masks.

In our simulation, the interactions among the carbon atoms in the graphene sheet are modelled by the Tersoff–Brenner empirical potential energy function [8–10]. The interactions between the argon atoms in the cluster and those between the carbon atoms and the argon atoms are modelled by the Lennard-Jones potential. The Tersoff–Brenner potential  $E_b$  is expressed as a summation of the binding energy over the atomic sites  $i$ :

$$E_b = \frac{1}{2} \sum_i E_i. \quad (1)$$

Thus, the force acting on atomic site  $i$  is given by

$$\vec{F}_i = -\frac{1}{2} \nabla_i \left( \sum_j E_j \right), \quad (2)$$

where  $\nabla_i = (\partial/\partial x_i, \partial/\partial y_i, \partial/\partial z_i)$ . The energy associated with atomic site  $i$  is expressed as the summation over the interaction potential between atom  $i$  and atom  $j$ :

$$E_i = \sum_{j(\neq i)} [V_R(r_{ij}) - \bar{B}_{ij} V_A(r_{ij})], \quad (3)$$

where  $r_{ij}$  is the distance between atom  $i$  and atom  $j$ . The functions  $V_R(r)$  and  $V_A(r)$  in equation (3) represent the Morse-type repulsive and attractive interactions, respectively, given by

$$V_R(r) = f(r_{ij}) \frac{D_e}{S-1} e^{-\beta\sqrt{2S}(r-R_e)}, \quad (4)$$

$$V_A(r) = f(r_{ij}) \frac{D_e S}{S-1} e^{-\beta\sqrt{2S}(r-R_e)}, \quad (5)$$

**Table 1.** C–C potential parameters.

$R_e$ (Å)	$D_e$ (eV)	$\beta$ (Å <sup>-1</sup> )	S	$\delta$
1.1315	6.325	1.5	1.29	0.804 69
$R_1$ (Å)	$R_2$ (Å)	$a_0$	$c_0$	$d_0$
1.7	2.0	0.011 304	19	2.5

**Table 2.** Lennard-Jones potential parameters.

$\epsilon_{Ar-Ar}$ (eV)	$\sigma_{Ar-Ar}$ (Å)	$\epsilon_{Ar-C}$ (eV)	$\sigma_{Ar-C}$ (Å)
0.0104	3.4	0.005	3.385

where  $f(r)$  is a smooth cutoff function:

$$f(r) = \begin{cases} 1 & r < R_1, \\ \frac{1}{2} \left( 1 + \cos \left[ \frac{r - R_1}{R_2 - R_1} \pi \right] \right), & R_1 < r < R_2, \\ 0, & r > R_2. \end{cases} \quad (6)$$

The function  $\bar{B}_{ij} \equiv (B_{ij} + B_{ji})/2$  in equation (3) represents the effect of a many-body coupling between bonds. The parameter  $B_{ij}$  is given by

$$B_{ij} = \left[ 1 + \sum_{k(\neq i, j)} G(\theta_{ijk}) f(r_{ik}) \right]^{-\delta}, \quad (7)$$

where  $\theta_{ijk}$  is the angle between bonds  $i-j$  and  $j-k$ , and the function  $G$  is given by

$$G(\theta) = a_0 \left[ 1 + \frac{c_0^2}{d_0^2} - \frac{c_0^2}{d_0^2 + (1 + \cos \theta)^2} \right]. \quad (8)$$

The set of parameters is shown in table 1. In Brenner's formula, a conjugate-compensation term exists; however, on the basis of the results of the previous study, it is ignored in our simulation [11].

The Lennard-Jones potential is given by

$$\phi(r) = 4\epsilon \left[ \left( \frac{\sigma}{r} \right)^{12} - \left( \frac{\sigma}{r} \right)^6 \right]. \quad (9)$$

The parameters for  $\epsilon$  and  $\sigma$  used in our simulation are shown in table 2 [11].

The position of the atom is updated by the velocity Verlet algorithm [12] with a time step of less than  $\Delta t = 0.3$  fs. To reduce the calculation time, we introduced a cutoff length. The interaction between argon atoms by a distance  $3.5\sigma_{Ar-Ar}$  or greater is neglected. The same cutoff is applied to the calculation of the van der Waals interaction between argon atom and carbon atom.

We assume that the argon cluster and the graphene sheet are in a low-temperature environment, and any thermostat is not used in our simulation.

### 3. Mechanical properties of graphene

The mechanical properties of graphene are important in studying the collision process between the argon cluster and

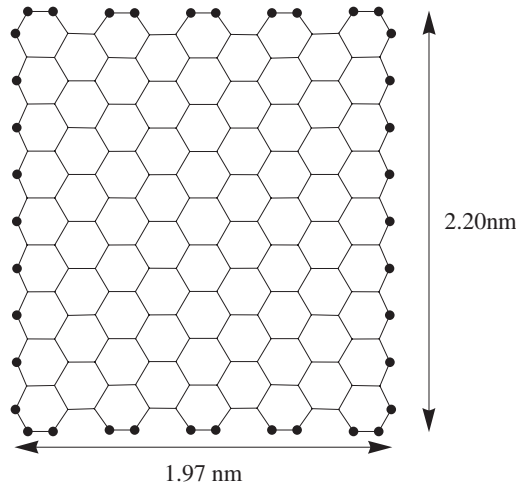


**Figure 2.** Illustration of the graphene sheet used in the simulation. Solid circles denote the fixed atoms.

the graphene sheet. Although the prediction of mechanical properties is not the aim of this paper, the bending rigidity  $D$  and fundamental frequency  $\nu_f$  are particularly important values when considering the dynamics of the graphene sheet in the following sections. Therefore, we calculate the fundamental frequency of the suspended nano-graphene shown in figure 2. This graphene sheet is nine six-membered carbon rings long and nine wide, and it contains a total of 190 atoms. We apply a boundary condition that the atoms shown by the solid circles in figure 2 are fixed in our simulation.

The fundamental frequency calculated by the MD method for small-amplitude oscillations is  $\nu_f = 4 \times 10^{11}$  Hz. This value is higher than the experimentally measured resonance frequency [5], because the size of the graphene sheet considered here is very small in comparison to that used in the experiments. In the experiment carried out by Bunch *et al*, the graphene sheets are suspended over a  $5 \mu\text{m}$  trench and the fundamental frequency varies from 1 to 170 MHz. Since the fundamental frequency of a rectangular membrane is in inverse proportion to the square of the side length, the fundamental frequency greatly increases by decreasing the size of the graphene sheet.

To estimate the bending rigidity of the graphene sheet using continuum mechanics, we assume that the graphene sheet is a square continuous membrane whose centre is the origin and that displacement  $w(x, y)$  satisfies the following boundary conditions:

$$\begin{aligned} w\left(\pm\frac{a}{2}, y\right) &= 0, & w\left(x, \pm\frac{b}{2}\right) &= 0, \\ \frac{\partial^2 w\left(\pm\frac{a}{2}, y\right)}{\partial x^2} &= 0, & \frac{\partial^2 w\left(x, \pm\frac{b}{2}\right)}{\partial y^2} &= 0, \end{aligned} \quad (10)$$

where  $a$  and  $b$  are the length and width of the membrane, respectively. According to the theory of elasticity [13], the fundamental eigenfrequency is given by

$$\nu_f = \frac{\pi}{2a} \sqrt{\frac{D\gamma}{M}} \left(1 + \frac{1}{\gamma^2}\right), \quad (11)$$

where  $M$  is the mass of the graphene and  $\gamma = b/a$  denotes the aspect ratio. Using this formula, we estimate the bending rigidity from the eigenfrequency to be 0.2 nN nm.

Let us consider the thickness of the membrane. Since the thickness of the graphene sheet is approximately that of a single carbon atom, it is difficult to define the thickness of the membrane. Therefore, the effective thickness is often used. The bending rigidity is represented using the thickness of the membrane  $h$ , the in-plane Young's modulus  $E$  and the in-plane Poisson's ratio  $\nu$  as

$$D = \frac{Eh^3}{12(1 - \nu^2)}. \quad (12)$$

Poot and Zant measured a value for the bending rigidity of several-layers-thick graphene, which closely agrees with that yielded by equation (12) in which the Young's modulus and Poisson's ratio assume the values of bulk graphite,  $E = 0.92$  TPa and  $\nu = 0.16$  [7]. Very recently, Lee *et al* reported that the two-dimensional second-order elastic stiffness of monolayer graphene is  $340 \text{ N m}^{-1}$  [14]. By dividing the interlayer spacing in graphite (0.335 nm), it yields an effective Young's modulus of  $E = 1.0$  TPa. They note that graphene is the strongest material ever measured. If the effective thickness is defined as the thickness that satisfies equation (12) and Young's modulus is 1.0 TPa, then it is 1.3 Å. This calculated value agrees with the thickness reported by Tserpes [15].

It is not very clear whether Young's modulus and Poisson's ratio of the single graphene layer are the same as those of bulk graphite. Young's modulus extracted by Frank *et al*,  $E = 0.5$  TPa, is indeed different from that of bulk graphite [16]. Therefore, further experimentation is required to determine the accurate mechanical properties of single-layer graphene; however, recent experiments have revealed that the graphene sheet becomes remarkably soft under a perpendicular force as the number of layers is decreased [7]. Thus, a single graphene sheet is an excellent candidate to act as a very soft and strong trampoline.

## 4. Simulation results

### 4.1. Collision with an argon atom

We now consider actuation of the graphene sheet occurring upon being struck by argon atoms. The most important parameters are the kinetic energy of the argon  $E_k$  and the size of the cluster. If the kinetic energy of the argon is significantly greater than the binding energy between the carbon atoms, the graphene sheet is ruptured by the impact. The threshold of kinetic energy required to rupture the graphene sheet depends on the impact position. Therefore, we randomly repositioned the point of impact inside a square region with sides of  $\sigma_{\text{Ar-Ar}}$  and observed whether or not the graphene was ruptured. If the kinetic energy of the cluster was less than 30 eV, which is almost four times the interaction energy per atom, the graphene did not rupture within a series of 100 trials. The graphene ruptured when the kinetic energy of the argon was 40 eV. Thus, the threshold of the kinetic energy is probably between 30 and 40 eV. When the graphene sheet ruptured, a small

hole was initially generated by the impact with the argon, which was later enlarged by the interaction between the carbon atoms. The process of rupturing is interesting; however, we concentrate our attention on the bending of the graphene sheet that does not result in its rupture.

The argon atom is initially located at  $z = -2\sigma_{\text{Ar-Ar}}$  independent of the kinetic energy of the cluster, and starts to move toward the graphene sheet with velocity  $v_z = \sqrt{2E_k/m_{\text{Ar}}}$  where the argon mass  $m_{\text{Ar}} = 6.6335 \times 10^{-26}$  kg. Figure 3(a) illustrates the change in the average maximum displacement  $z_{\text{max}}$  over 100 trials for  $E_k = 10, 20$  and  $30$  eV. The initial velocities are  $v_z = 6.95$  km s $^{-1}$ ,  $9.83$  km s $^{-1}$  and  $12.0$  km s $^{-1}$  for  $E_k = 10, 20$  and  $30$  eV, respectively. The graphene sheet is deformed by the impact in a very short time, and the displacements of the atoms near the centre reach their maximum values in less than 1 ps. The maximum displacement increases with kinetic energy. The maximum forces generated by the impact are approximately 4, 8 and 10 nN for  $E_k = 10, 20$  and  $30$  eV, respectively. The argon atom loses its kinetic energy quickly, in less than 2 fs. If the velocity decreases to zero within the interval  $\Delta t = 2$  fs, the mean forces acting on the argon, roughly estimated by  $m_{\text{Ar}}v_z/\Delta t$ , are 4.6, 6.5 and 8 nN for  $E_k = 10, 20$  and  $30$  eV, respectively. The time required for the argon to transfer its kinetic energy to the graphene sheet is significantly smaller than the eigenperiod of the graphene sheet. Accordingly, the force acting on the graphene sheet is regarded as an impulsive force.

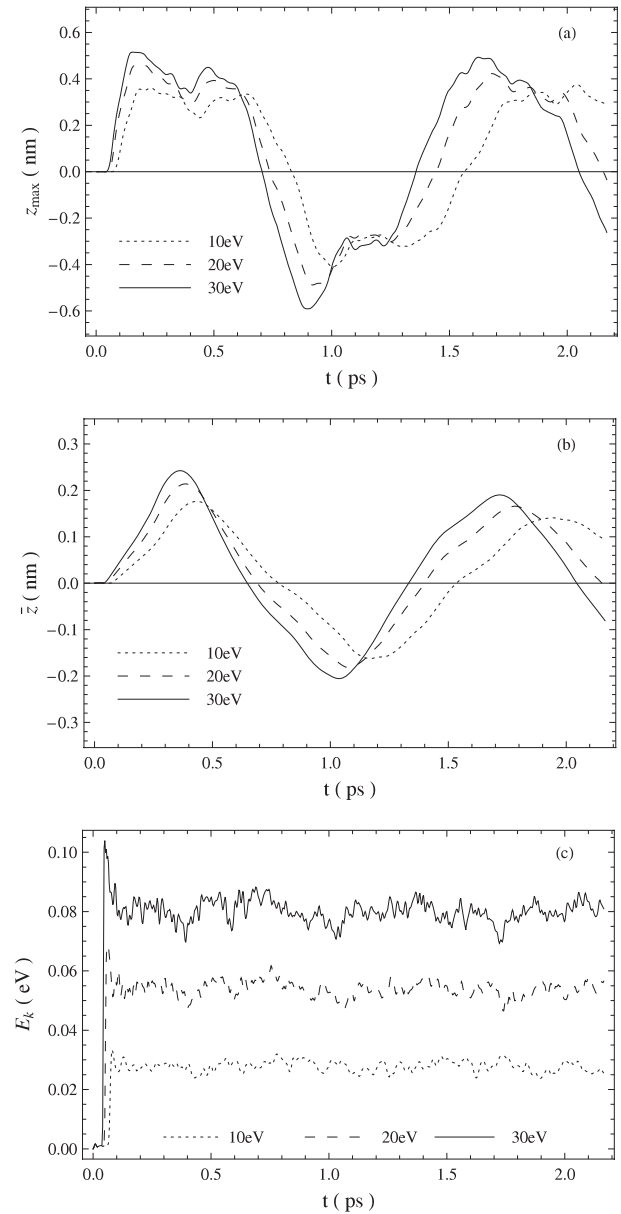
In addition to the maximum displacement, the mean of the displacement  $\bar{z}$  that is averaged over all atoms is important. Figure 3(b) shows the mean of the displacement under the same conditions used for figure 3(a). Note that the averaged mean displacement reaches its maximum value after the appearance of the first peak of the averaged maximum displacement. This is because the deformation spreads from the centre to the edge of the graphene sheet.

Figure 3(c) shows the kinetic energy of the graphene per carbon atom  $E_k$ . Although the graphene sheet oscillates vertically, the fluctuation of the kinetic energy of the graphene sheet is small. This is because the contribution concerning the vertical velocity to the total kinetic energy is small. In other words, the kinetic energy of the argon cluster is transferred mainly to the horizontal oscillations of the carbon atoms, namely heat.

#### 4.2. Collision with an argon cluster

Gas cluster ion beams have many potential uses in the field of surface processing, such as in dry etching, surface cleaning and surface smoothing [17]. The gas cluster is a good carrier of kinetic energy. In contrast to a monomer ion beam, the kinetic energy per atom in the cluster can be decreased without decreasing the total kinetic energy, simply by increasing the number of atoms in the cluster. This enables low-damage, atomic-scale surface smoothing and shallow implantation.

An argon cluster consisting of 10 atoms was made to collide vertically with the graphene sheet. The argon cluster initially had the lowest potential [18] and its centre of mass was located at  $(x, y, z) = (0, 0, -2\sigma_{\text{Ar-Ar}})$ . The mean radius



**Figure 3.** Plot of the temporal changes in the displacement of the graphene sheet caused by a single argon atom: (a) average maximum displacement, (b) average mean displacement and (c) kinetic energy of the graphene sheet per carbon atom for three different kinetic energy values of the argon atom (10, 20 and 30 eV).

of the cluster was 0.33 nm. The displacement of the graphene sheet after collision was dependent on the configuration of atoms in the cluster. Therefore, we calculated the average value of various displacements of the graphene sheet that occurred through collisions with different configurations of atoms in the cluster.

The values of the averaged maximum displacement and averaged mean displacement of the graphene sheet recorded for collisions for over 100 different configurations of the argon cluster are illustrated in figures 4(a) and (b), respectively, for  $E_k = 50, 100$  and  $150$  eV. Both figures clearly show that collision with an argon cluster resulted in greater deformation of the graphene sheet than did collision with a single atom. The

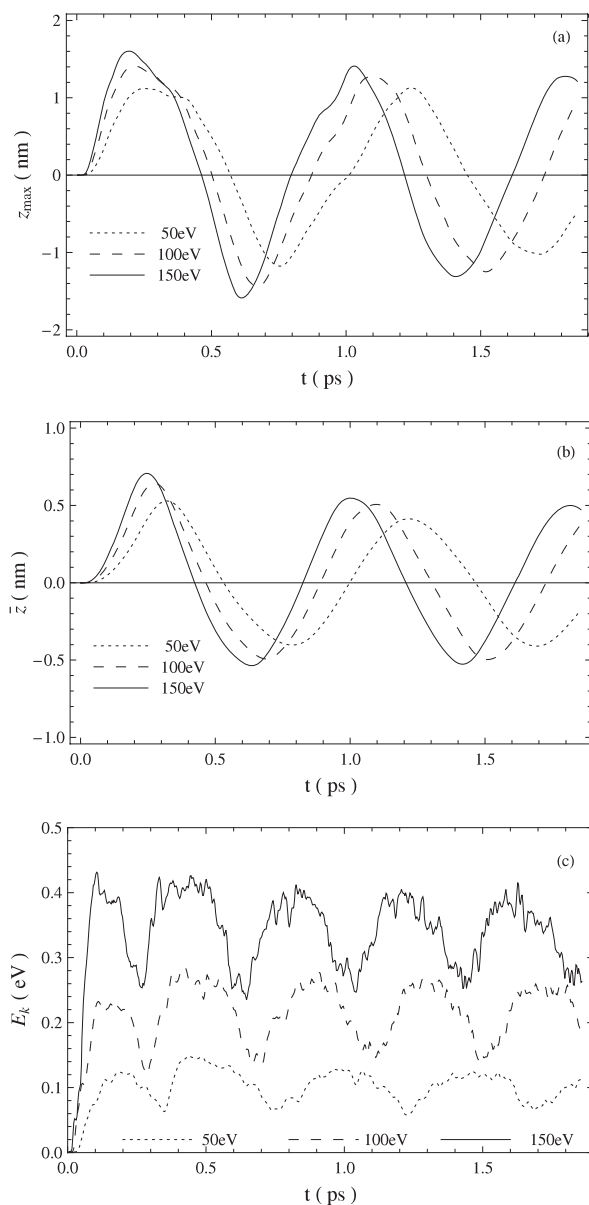


**Figure 4.** Plot of the temporal changes in the displacement of the graphene sheet caused by an argon cluster containing 10 atoms: (a) averaged maximum displacement, (b) averaged mean displacement and (c) kinetic energy of the graphene sheet per carbon atom for three different kinetic energy values of the argon cluster (50, 100 and 150 eV).

displacement caused by the collision with the cluster is almost three times larger than that by a monomer. The total kinetic energy of the cluster is greater than that of a single argon atom; however, the kinetic energy per atom is close to that used in the monomer simulation; the risk of rupturing the graphene sheet does not increase much.

We expect the extent of deformation to increase with the size of the graphene sheet and of the cluster. As an example, we simulate the collision of an argon cluster containing 1000 atoms with a graphene sheet consisting of  $51 \times 45$  six-member carbon rings. The length and width of the graphene sheet are 11.0 nm and 10.9 nm, respectively. Figure 5 shows the temporal change in the displacement of the graphene sheet

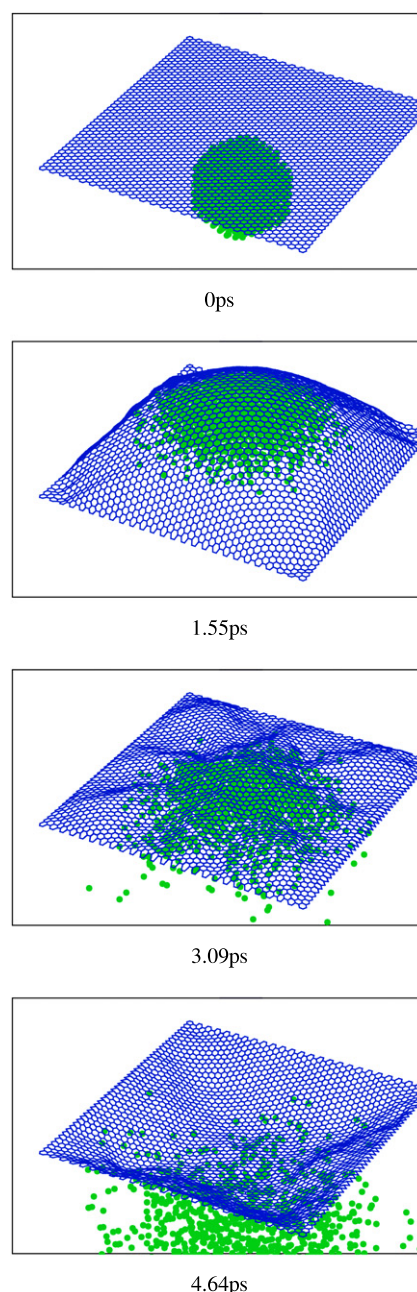


**Figure 5.** Deformation of a graphene sheet containing 4732 carbon atoms during impact with a cluster containing 1000 argon atoms. The kinetic energy of the argon cluster is 5 keV.

caused by collision with the argon cluster whose kinetic energy is 5 keV. The dome-shaped graphene sheet is found at 5 ps. The maximum height and volume of the dome are 4 nm and  $3 \text{ nm}^3$ , respectively. It is noteworthy that no argon atoms penetrate the graphene sheet.

Figure 4(c) shows the kinetic energy of graphene per carbon atom after the collision of the argon cluster. By comparison with figure 3(c), both the absolute values and fluctuations of the kinetic energy of graphene shown in figure 4(c) are larger than those in figure 3(c). This means that the larger amount of energy can be transferred to the graphene sheet by using argon clusters.

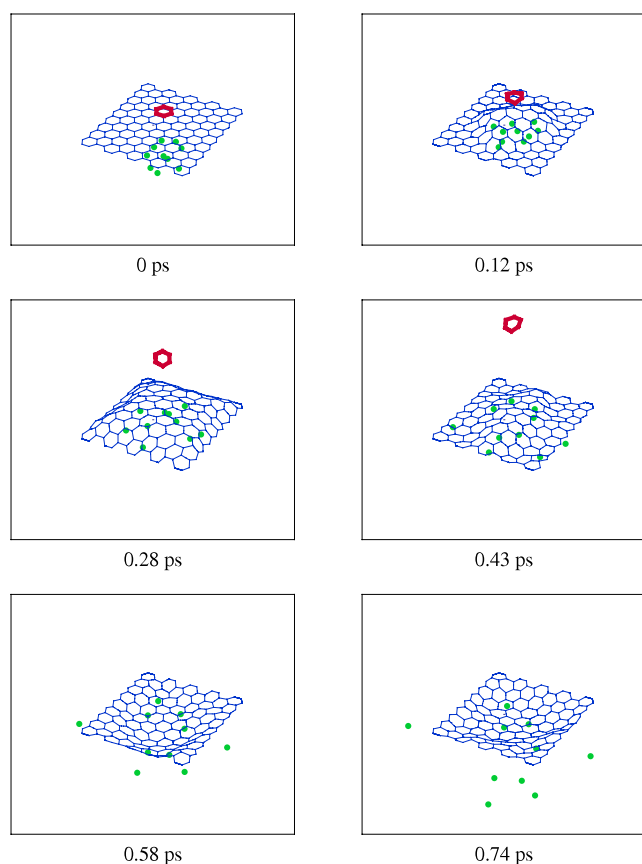


**Figure 6.** Illustration of molecular ejection by rapid movement of a six-member carbon ring.

## 5. Application of the actuator to molecular ejection

When the argon cluster collides with the graphene sheet, it causes the sheet to bend quickly. As an application of this actuation, we consider the ejection of a molecule that bonds weakly with the graphene. If the binding energy between the atoms in the molecule  $\epsilon_{M-M}$  is significantly greater than that between the molecule and the graphene  $\epsilon_{M-G}$ , the molecule is released by providing energy between  $\epsilon_{M-M}$  and  $\epsilon_{M-G}$  to the molecule without causing it to break. This technique may be used in mass spectrometry, nanosurface chemistry and molecular printing.

Figure 6 shows a demonstration of molecular ejection by the impact of an argon cluster with a graphene sheet. An argon cluster contains 10 atoms and its kinetic energy is 100 eV. A six-member carbon ring is located on the graphene sheet with a separation of 3.4 Å, which corresponds to the gap between graphene sheets found in graphite. We assume that the interaction between the graphene sheet and the six-member carbon ring is modelled by the Lennard-Jones potential with parameters  $\epsilon_{C-G} = 0.00188$  eV and  $\sigma_{C-G} = 3.33264$  Å [19]. This binding energy  $\epsilon_{C-G}$  is significantly smaller than that between carbon atoms in the six-member carbon ring.

Two forces act on the six-member carbon ring when the collision between the graphene sheet and the argon cluster occurs. The first force is the attractive force between the carbon atoms in the six-member carbon ring and the argon atoms. The

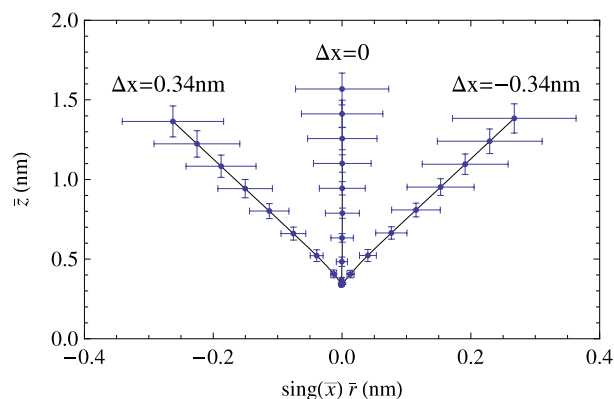


**Figure 7.** Plot of the trajectories of the ejected six-member carbon ring for three impact positions. The gap between the centre of the six-member carbon ring and the centre of mass of the argon cluster at  $t = 0$  is denoted by  $\Delta x$ .

second force is the repulsive force between the carbon atoms in the six-member carbon ring and the carbon atoms in the graphene sheet. The repulsive force between the carbon atoms rapidly increases as the graphene sheet approaches the six-member carbon ring. This repulsive force is greater than the attractive force, causing it to be released from the surface of the graphene sheet. If the kinetic energy is insufficient to cut the binding between the graphene sheet and the six-member carbon ring, the six-member carbon ring stays in its position relative to the graphene sheet and does not leave the graphene sheet.

The trajectory of the carbon ring depends on the position where the argon cluster collides with the graphene sheet. We set the initial position of the centre of the argon cluster at  $(\Delta x, 0, -2\sigma_{Ar-Ar})$  and consider the influence of the gap  $\Delta x$  on the trajectory of the carbon ring. The other parameters are the same as those used in the previous simulation for ejection. Figure 7 shows the trajectories of the carbon rings which are averaged over 100 different configurations of the argon cluster for three different gaps. The horizontal axis denotes  $\text{sgn}(\bar{x})\bar{r}$ , where  $\bar{x}$  denotes the mean position along the  $x$  axis and  $\bar{r}$  denotes the mean distance from the centre of mass of the carbon ring before the collision. To indicate the direction of the ejection, the function  $\text{sgn}(x)$  that denotes the sign of  $x$  is used. The vertical axis denotes the mean position along the  $z$  axis. The horizontal and vertical bars attached to the points in the figure denote the standard deviation of the position. Figure 7 illustrates that, if the argon cluster collides on the left-hand side of the carbon ring, the carbon ring is ejected to the right-hand side. Conversely, if the argon cluster collides on the right-hand side of the carbon ring, the carbon ring is ejected to the left. Therefore, the direction of ejection can be roughly controlled by changing the axis of the argon cluster beam.

## 6. Conclusions

We have proposed a simple method of actuating a graphene sheet. The recent remarkable progress of gas cluster ion beam technology has enabled us to obtain argon clusters whose size

and velocity are controlled very precisely. Therefore, it is possible to realize our proposal by using currently available technology.

Although MD simulation often requires a long calculation time, it is used in this study to examine the actuation of a graphene sheet because it is difficult to otherwise analyse the collision of the argon cluster with the graphene sheet. In particular, the advantage of MD is that the effect when the argon cluster is broken apart is correctly simulated.

A more precise prediction of the dynamics of the graphene sheet calls for some modifications to the simulation. First, the boundary conditions must be changed. In our simulation, the atoms on the edge of the graphene sheet were fixed; however, in reality, the graphene sheet is peeled from the substrate by the impact. Second, the lattice vibration of the substrate must be taken into account when future simulations are performed.

As an application of our proposal, we considered molecular ejection from the graphene sheet. Though this desorption is essential in molecular manipulation, it is more difficult than adsorption of the molecule onto the graphene surface. Using our method, the molecule is desorbed without being directly touched, unlike manipulation using atomic force microscopy. In addition, the cluster beams can actuate many suspended graphene sheets simultaneously.

## Acknowledgments

The authors would like to thank Michihiro Hashinokuchi and Nobuyasu Ito for helpful discussions.

## References

- [1] Novoselov K S, Geim A K, Morozov S V, Jiang D, Zhang Y, Dubonos S V, Grigorieva I V and Firsov A A 2004 *Science* **306** 666
- [2] Novoselov K S, Geim A K, Morozov S V, Jiang D, Zhang Y, Dubonos S V, Grigorieva I V and Firsov A A 2005 *Nature* **438** 197
- [3] Schedin F, Geim A K, Morozov S V, Hill E W, Blake P, Katsnelson M I and Novoselov K S 2007 *Nat. Mater.* **6** 652
- [4] Meyer J C, Geim A K, Katsnelson M I, Novoselov K S, Booth T J and Roth S 2007 *Nature* **446** 60
- [5] Bunch L S, van der Zande A M, Verbridge S S, Frank I W, Tanenbaum D M, Parpia J M, Craighead H G and McEuen P L 2007 *Science* **315** 490
- [6] Heermann D W 1986 *Computer Simulation Methods* (Philadelphia: Springer)
- [7] Poot M and van der Zant H S J 2008 *Appl. Phys. Lett.* **92** 063111
- [8] Brenner D W 1990 *Phys. Rev. B* **42** 9458
- [9] Brenner D W, Shenderova O A, Harrison J A, Stuart S J, Ni B and Sinnott S B 2002 *J. Phys.: Condens. Matter* **14** 783
- [10] Zhou J and Huang R 2008 *J. Mech. Phys. Solids* **56** 1609
- [11] Yamaguchi Y and Gspann J 2001 *Eur. Phys. J. D* **16** 103
- [12] Verlet L 1967 *Phys. Rev.* **98** 159
- [13] Landau L D and Lifshitz E M 1986 *Theory of Elasticity* (Oxford: Butterworth-Heinemann)
- [14] Lee C, Wei X, Kysr J W and Hone J 2008 *Science* **231** 385
- [15] Tserpes K I and Papanikos P 2005 *Composites B* **36** 468
- [16] Frank I W, Tanenbaum D M, van der Zande A M and McEuen P L 2007 *J. Vac. Sci. Technol. B* **25** 2558
- [17] Yamada I, Matsuo J, Toyoda N and Kirkpatrick A 2001 *Mater. Sci. Rep.* **34** 231
- [18] Wales D J and Doye J P K 1997 *J. Phys. Chem. A* **101** 5111
- [19] Wang Y, Scheerschmidt K and Gösele U 2000 *Phys. Rev. B* **61** 12864